freeze-thawing PVA remarkably diminished after 292 s running as shown in Figure 10, and therefore the fluid load support became small (Figure 11). The friction in saline is expected to increase gradually as indicated by the curve for $\mu_{solid} = 0.2$ (Figure 12). Even in case of low fluid load support, it was demonstrated in experiment that another lubrication mechanism as boundary lubrication with important synovia constituents enables to reduce friction remarkably (Figures 7 to 9) and minimize wear (Figure 9). The comparison of experimental results (Figures 6 to 8) with biphasic FE analysis (Figure 12) clearly demonstrates the acceptable correspondence of both cases for high or low friction by considering appropriate selection of 0.2 or 0.01 as μ_{solid}. Therefore, it is indicated that the usage of freeze-thawing PVA lubricated with a simulated synovial fluid is a possible solution for clinical application.

Next, the friction behaviours of the cast-drying PVA hydrogel should be considered. As shown in Figure 6, the low friction of cast-drying PVA hydrogel during sliding duration in saline for a long time is very attractive. This property appears to be derived from low permeability (Table 1) of biphasic material. As shown in Figure 10, the interstitial fluid pressure sustained even after 292 s running for cast-drying PVA. Its fluid load support increased after 292 s running for $\mu_{solid} = 0.2$ (Figure 11). Therefore, friction can be reduced after 292 s running for $\mu_{solid} = 0.2$ in biphasic analysis (Figure 12). However, the frictional behaviour in experiment (Figure 6) is different from the estimated curves for $\mu_{solid} = 0.2$ or 0.01. The appropriate selection for $\mu_{solid} = 0.05$ or so may bring favourable correspondence.

Thus, it is worthy of remark that the permeability regulated by the material properties and structures of hydrogel will mainly control the biphasic fluid flow behaviour. The material properties and structures in both PVA hydrogels appear to depend on the structure controlled by hydrogen bond. The model for microstructure in PVA hydrogel was proposed by Otsuka and Suzuki[38] as shown in Figure 13.

The formation of hydrogen bonds and microcrystallites was identified using X-ray diffraction (XRD) technique, Fourier transform infrared (FTIR) spectroscopy and measurements of the swelling ratio under repeated water exchanges.[43] In Figure 13, d, D and L are deduced from the diffraction peaks at XRD spectra. Small-angle scattering indicates that the distance between microcrystallites L in freeze-thawing PVA hydrogel is shorter than in cast-drying PVA hydrogel. As shown in Figure 1, the transparency of cast-drying hydrogel indicates its uniform network structure, and the milky white appearance of freezing-thawing hydrogel suggests the heterogeneous network structure. In Figure 14, the schematic models based on personal communication from E Otsuka and A Suzuki[42] for these hydrogels are shown accompanied with atomic force microscopy (AFM) surface images of their swollen states in water. The network

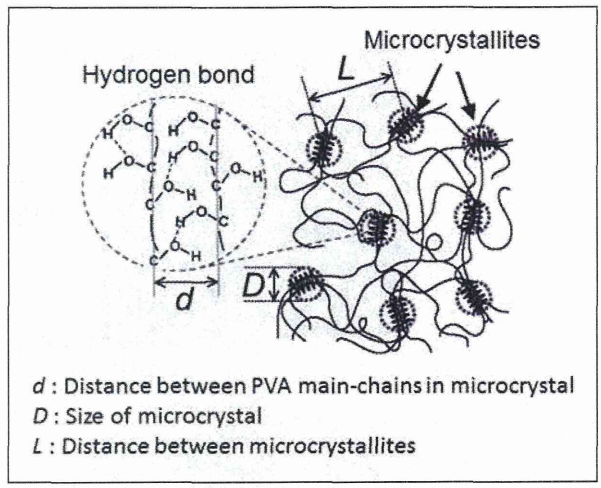

Figure 13. Network structure of PVA hydrogels crosslinked by microcrystallites.[38]
PVA: poly(vinyl alcohol).
Source: reproduced with permission of John Wiley & Sons, Inc.

is generally composed of microcrystallites and amorphous zones. It is suggested that the fluid flows out rapidly from freeze-thawing PVA hydrogel, which is composed of microcrystallites and considerable amorphous zones, as indicated by high permeability (Table 1), and porous texture in AFM image (Figure 14). On the contrary, in cast-drying PVA hydrogel with low permeability, the fluid retained inside of gel with slow flows out, and thus the interstitial fluid pressure maintains for longer time under reciprocating tests.

Friction for biphasic materials under lubricated conditions is estimated from a combination of the friction for solid-to-solid contact and the negligibly low friction for fluid load support, as indicated in formula for friction by Ateshian et al.,[44,45] where high partitioning of load support by fluid phase contributes to lowering in friction. Changes in load support in compliant hydrogels estimated on the basis of biphasic FE analysis for reciprocating test under continuous loading are shown in Figure 11, which depend on not only permeability but also friction level for solid-to-solid contact. In saline where the friction for solid-to-solid contact is high, the higher load support by interstitial fluid pressure maintained with low permeability for cast-drying gel gives lower friction, while the limited load support by low-fluid pressure attributable to faster fluid exudation caused by higher permeability for repeated freeze-thawing gel gives high friction, as shown in Figure 12. The lower friction for cast-drying gel in saline (Figure 6) appears to be brought about by superior surface lubricity as $\mu_{solid} = 0.05$ or so as mentioned above. The smooth surface of cast-drying PVA may contribute to the reduction of friction in saline by suppressing interaction between rubbing surfaces. The rough and porous surface of freeze-thawing PVA may enhance interaction between rubbing surfaces in saline and

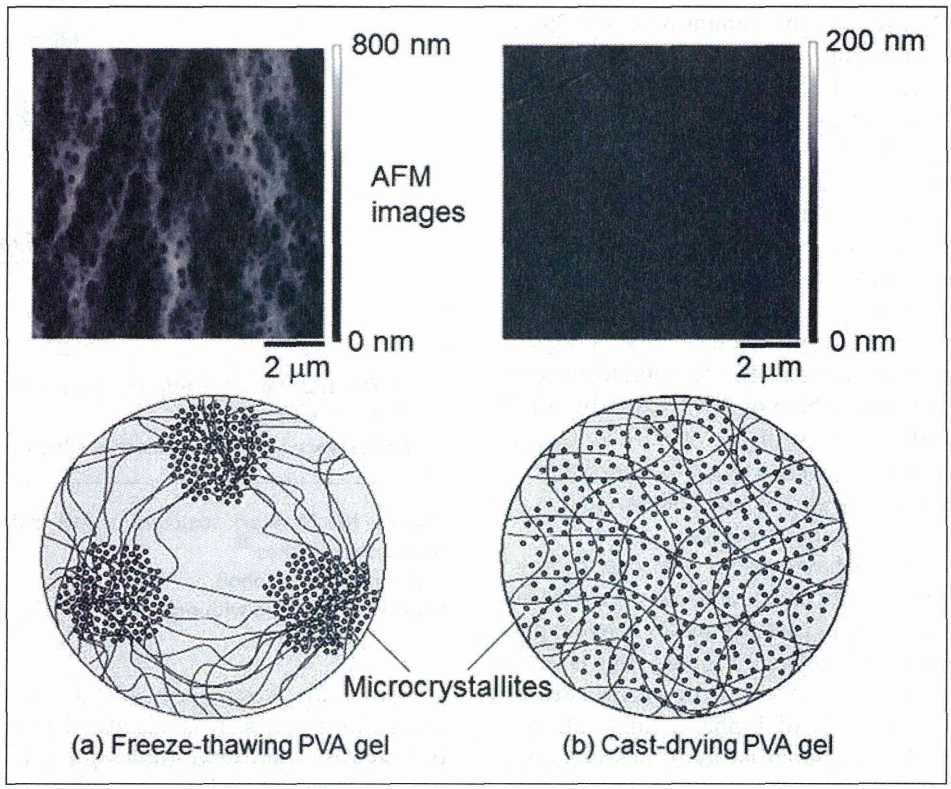

Figure 14. AFM images in water and schematic models[42] for two kinds of hydrogel structures. AFM: atomic force microscopy.

increase friction, but improve the adsorbed film formation under lubricated condition with a simulated synovial fluid and reduce friction (Figures 8, 9 and 12). Elucidation of the exact lubrication mechanism for hydrogel should be continued in further studies.

Other improving methods for properties of PVA hydrogel are to additionally control the nanoscopic structure, to reinforce the structure with fibrous element or other method and thus to enhance biphasic properties for efficient lubrication and load-carrying property. The freeze-thawing and cast-drying PVA hydrogels based on hydrogen-bonding network as physical bonding prepared without any additives or irradiative stimulus have superiority in safety in human body. The possibility of restoration with hydrogen bonding in case of local fracture is a favourable property.

The main purpose of this study was to examine friction differences between two kinds of hydrogels, but wear differences become more important in clinical application. In authors' related research on reciprocating tests with an alumina ball against flat PVA hydrogel plates in pure water (Suzuki et al.[46]), cast-drying gel with low permeability showed lower wear and lower friction than freeze-thawing gel with high permeability. The superiority of cast-drying gel appears to be caused by its better biphasic property in water. However, in this study, freeze-thawing gel exhibited minimum wear in simulated synovia lubricant as HA solution containing appropriate concentration of albumin, γ-globulin and DPPC in reciprocating tests under continuous loading. This indicates the effectiveness of surface protection by adsorbed film formed on freeze-thawing gel surface. The wear behaviour of cast-drying gel in various lubricants should be examined in future studies.

For the clinical application of PVA hydrogel, durability, synergistic interaction with lubricants, ease of production, formability, appropriate fixation methods and other properties are required. In particular, the establishment of appropriate design in consideration of a multimode lubrication mechanism is required not only for low friction but also for zero-wear and high-fatigue resistance in the human body. To evaluate predictively the in vivo behaviours of two kinds of hydrogels, the various tests such as reciprocating tests and simulator tests should be conducted under biomechanically simulated environmental conditions. The desirable in vivo performance of PVA hydrogel implanted in rabbit knee joint in ongoing tests with biomedical research group suggests the feasibility of clinical application. In the next step, the authors plan to apply a hybrid hydrogel (Suzuki et al.[46]) composed of cast-drying PVA on freeze-thawing PVA as another candidate material for the artificial cartilage with superior lubricity.

Conclusion

To explore the superior lubricity of articular cartilage and artificial hydrogel cartilage, time-dependent frictional behaviours in natural articular cartilage and

two kinds of PVA hydrogels prepared by repeated freeze-thawing method and cast-drying method were examined in reciprocating tests and biphasic FE analyses.

Articular cartilage showed initial low friction and gradual increase in saline lubrication where biphasic fluid load support mechanism subsides with rubbing as indicated by biphasic FE analysis. However, the addition of a simulated synovial fluid enabled the superior lubrication by appropriate adsorbed film formation in boundary lubrication mode.

In artificial cartilage materials in saline, cast-drying PVA with low permeability clearly showed significantly lower friction than freeze-thawing PVA with high permeability. For freeze-thawing PVA hydrogel in which biphasic lubrication mechanism diminished with rubbing, the supply of appropriate synovia constituents improved friction and wear properties in boundary lubrication mode.

It was shown that the synergistic combination of biphasic lubrication and boundary lubrication becomes effective to sustain superior lubricity in articular cartilage and PVA hydrogels even at slow movement under continuous loading.

Funding

The authors thank the financial support given by the Grant-in-Aid for Specially Promoted Research of Japan Society for the Promotion of Science (Kaken: 23000011).

References

1. Dowson D. Modes of lubrication in human joints. *Proc IMechE* 1966–1967; 181(Pt 3J): 45–54.
2. Unsworth A, Dowson D and Wright V. Some new evidence on human joint lubrication. *Ann Rheum Dis* 1975; 34(4): 277–285.
3. Murakami T. The lubrication in natural synovial joints and joint prostheses. *JSME Int J Ser III* 1990; 33(4): 465–474.
4. Dowson D and Jin ZM. Micro-elastohydrodynamic lubrication of synovial joints. *Eng Med* 1986; 15: 65–67.
5. Forster H and Fisher J. The influence of loading time and lubricant on the friction of articular cartilage. *Proc IMechE Part H: J Engineering in Medicine* 1996; 210: 109–119.
6. Ateshian GA. Theoretical formulation for boundary friction in articular cartilage. *J Biomech Eng* 1997; 119(1): 81–86.
7. Klein J. Molecular mechanisms of synovial joint lubrication. *Proc IMechE Part J: J Engineering Tribology* 2006; 220: 691–710.
8. Ikeuchi K. Origin and future of hydration lubrication. *Proc IMechE Part J: J Engineering in Medicine* 2007; 221: 301–305.
9. Swann DA, Hendren RB, Radin EL, et al. The lubricating activity of synovial fluid glycoproteins. *Arthrit Rheum* 1981; 24: 22–30.
10. Hills BA. Oligolamellar lubrication of joints by surface active phospholipids. *J Rheum* 1989; 16(1): 82–91.
11. Higaki H and Murakami T. Role of constituents in synovial fluid and surface layer of articular cartilage in joint lubrication (part 2) the boundary lubricating ability of proteins. *Jpn J Tribol* 1996; 40(7): 691–699.
12. Murakami T, Sawae Y, Horimoto M, et al. Role of surface layers of natural and artificial cartilage in thin film lubrication. In: D Dowson, M Priest, CM Taylor, et al. (eds) *Lubrication at the frontier*. Amsterdam: Elsevier, 1999, pp.737–747.
13. Murakami T, Higaki H, Sawae Y, et al. Adaptive multimode lubrication in natural synovial joints and artificial joints. *Proc IMechE, Part H: J Engineering in Medicine* 1998; 212: 23–35.
14. Murakami T. Importance of adaptive multimode lubrication mechanism in natural and artificial joints. *Proc IMechE Part J: J Engineering Tribology* 2012; 226: 827–837.
15. Murakami T, Nakashima K, Yarimitsu S, et al. Effectiveness of adsorbed film and gel layer in hydration lubrication as adaptive multimode lubrication mechanism for articular cartilage. *Proc IMechE Part J: J Engineering Tribology* 2011; 225: 1174–1185.
16. Murakami T, Yarimitsu S, Nakashima K, et al. Influence of synovia constituents on tribological behaviors of articular cartilage. *Friction* 2013; 1(2): 150–162.
17. Sakai N, Hagihara Y, Furusawa T, et al. Analysis of biphasic lubrication of articular cartilage loaded by cylindrical indenter. *Tribol Int* 2012; 46: 225–236.
18. Hosoda N, Sakai N, Sawae Y, et al. Depth-dependence and time-dependence in mechanical behavior of articular cartilage in unconfined compression test under constant total deformation. *J Biomech Sci Eng* 2008; 3: 209–220.
19. Li LP, Soulhat J, Buschmann MD, et al. Nonlinear analysis of cartilage in unconfined ramp compression using a fibril reinforced poroelastic model. *Clin Biomech* 1999; 14: 673–682.
20. Willert HJ and Semlitsch M. Reaction of the articular capsule to wear products of artificial joint prostheses. *J Biomed Mater Res* 1977; 11: 157–164.
21. Ingham E and Fisher J. The role of macrophages in osteolysis of total joint replacement. *Biomaterials* 2005; 26: 1271–1286.
22. Williams PA, Yamamoto K, Masaoka T, et al. Highly crosslinked polyethylenes in hip replacements: improved wear performance or paradox? *Tribol Trans* 2007; 50: 277–290.
23. Tomita N, Kitakura T, Onmori N, et al. Prevention of fatigue cracks in ultrahigh molecular weight polyethylene joint components by the addition of vitamin E. *J Biomed Mater Res (Appl Biomater)* 1999; 48: 474–478.
24. Moro T, Takatori Y, Ishihara K, et al. Surface grafting of artificial joints with a biocompatible polymer for preventing periprosthetic osteolysis. *Nat Mater* 2004; 3: 829–836.
25. Dowson D. Are our joint replacement materials adequate? In: *Proceedings of the IMechE International Conference*, 1989, C384/KN1: 1–5.
26. Unsworth A, Pearcy MJ, White EFT, et al. Soft layer lubrication of artificial hip joints. *Proc IMechE* 1987; C219/87: 715–724.
27. Murakami T, Ohtsuki N and Higaki H. The adaptive multimode lubrication in knee prostheses with compliant layer during walking motion. In: D Dowson, et al.

(eds) *Thin films in tribology. Tribology series 25.* Elsevier, 1993, pp.673–682.
28. Sasada T. Biomechanics and biomaterials—friction behaviour of an artificial articular cartilage. In: *Transactions of 3rd World Biomaterials Congress*, Kyoto, 1988, vol. 11, p.6.
29. Oka M, Ushio K, Kumar K, et al. Development of artificial cartilage. *Proc IMechE, Part H: J Engineering in Medicine* 2000; 214: 59–68.
30. Kobayashi M and Hyon SH. Development and evaluation of polyvinyl alcohol-hydrogels as an artificial articular cartilage for orthopedic implants. *Materials* 2010; 3: 2753–2771.
31. Murakami T, Sawae Y, Higaki H, et al. The adaptive multimode lubrication in knee prostheses with artificial cartilage during walking. In: Dowson, et al. (eds) *Elastohydrodynamics '96: fundamentals and applications in lubrication and traction.* Elsevier Science, 1997, pp.383–394.
32. Murakami T, Sawae Y, Nakashima K, et al. Tribological behaviours of artificial cartilage in thin film lubrication. In: D Dowson, et al. (eds) *Thinning films and tribological interfaces. Tribology and Interface Engineering Series 38.* Elsevier Sciences, 2000, pp.317–327.
33. Nakashima K, Sawae Y and Murakami T. Study on wear reduction mechanisms of artificial cartilage by synergistic protein boundary film formation. *JSME Int J* 2005; 48(4): 555–561.
34. Yarimitsu S, Nakashima K, Sawae Y, et al. Influences of lubricant composition on forming boundary film composed of synovia constituents. *Tribol Int* 2009; 42: 1615–1623.
35. Corkhill PH, Trevett AS and Tighe BJ. Potential of hydrogels as synthetic articular cartilage. *Proc IMech E Part H: J Engineering in Medicine* 1990; 204: 147–155.
36. Arakaki K, Kitamura N, Fujiki H, et al. Artificial cartilage made from a novel double-network hydrogel: in vivo effects on the normal cartilage and ex vivo evaluation of the friction property. *J Biomed Mater Res Part A* 2010; 91: 1160–1168.
37. Nakashima K, Murakami T and Sawae Y. Evaluation of tribological properties of polyvinyl alcohol hydrogel as artificial cartilage. In: *Proceedings of the international tribology conference*, Nagasaki, 2000, vol. 2, pp.1537–1540.
38. Otsuka E and Suzuki A. A simple method to obtain a swollen PVA gel crosslinked by hydrogen bonds. *J Appl Polym Sci* 2009; 114(1): 10–16.
39. Otsuka E, Sugiyama M and Suzuki A. Network microstructure of PVA cast gels observed by SAXS measurements. *J Phys* 2010; conf. Ser. 247: 012043.
40. Jurvelin JS, Bushmann MD and Hunziker EB. Mechanical anisotropy of the human knee articular cartilage in compression. *Proc IMechE: J Engineering in Medicine* 2003; 217: 215–219.
41. Yamaguchi T and Murakami T. Surface friction and bulk transport properties in hydrogels. *Prepr JAST Conf* 2013; 9: 199–200.
42. Murakami T, Yarimitsu Y, Nakashima K, et al. Time-dependent frictional behaviors in hydrogel artificial cartilage materials. In: *Proceedings of the sixth international biotribology forum*, Fukuoka, 2011, pp.65–68.
43. Otsuka E and Suzuki A. Swelling properties of physically cross-linked PVA gels prepared by a cast-drying method. *Prog Colloid Polym Sci* 2009; 136: 121–126.
44. Ateshian GA, Wang H and Lai WM. The role of interstitial fluid pressurization and surface porosities on the boundary friction of articular cartilage. *ASME J Tribol* 1998; 120: 241–248.
45. Ateshian GA. The role of interstitial fluid pressurization in articular cartilage lubrication. *J Biomech* 2009; 42: 1163–1176.
46. Suzuki A, Sasaki S, Sasaki S, et al. Elution and wear of PVA hydrogels by reciprocating friction. Extended abstract for: *World tribology congress 2013*, Torino [on USB].

Appendix

Notation

C	constant
$f(t)$	compressive stress during stress relaxation
G	shear modulus of rigidity
k	permeability
K	bulk modulus of elasticity
t	time
t_{rel}	relaxation time
W	shorter width of specimen
ε_{z0}	compressive strain
μ_{solid}	friction coefficient for solid-to-solid contact

Society For Biomaterials

Effect of UV-irradiation intensity on graft polymerization of 2-methacryloyloxyethyl phosphorylcholine on orthopedic bearing substrate

Masayuki Kyomoto,[1,2,3] Toru Moro,[2,4] Shihori Yamane,[2,3] Masami Hashimoto,[5] Yoshio Takatori,[2,4] Kazuhiko Ishihara[1]

[1]Department of Materials Engineering, School of Engineering, The University of Tokyo, 7-3-1 Hongo, Bunkyo-ku, Tokyo 113-8656, Japan
[2]Division of Science for Joint Reconstruction, Graduate School of Medicine, The University of Tokyo, 7-3-1 Hongo, Bunkyo-ku, Tokyo 113-8656, Japan
[3]Research Department, KYOCERA Medical Corporation, 3-3-31, Miyahara, Yodogawa-ku, Osaka 532-0003, Japan
[4]Sensory and Motor System Medicine, Faculty of Medicine, The University of Tokyo, 7-3-1 Hongo, Bunkyo-ku, Tokyo 113-8655, Japan
[5]Materials Research and Development Laboratory, Japan Fine Ceramics Center, 2-4-1 Mutsuno,, Atsuta-ku, Nagoya 456-8587, Japan

Received 9 September 2013; accepted 24 September 2013
Published online 00 Month 2013 in Wiley Online Library (wileyonlinelibrary.com). DOI: 10.1002/jbm.a.34973

Abstract: Photoinduced grafting of 2-methacryloyloxyethyl phosphorylcholine (MPC) onto cross-linked polyethylene (CLPE) was investigated for its ability to reduce the wear of orthopedic bearings. We investigated the effect of UV-irradiation intensity on the extent of poly(MPC) (PMPC) grafting, and found that it increased with increasing intensity up to 7.5 mW/cm^2, and the remained fairly constant. It was found to be extremely important to carefully control the UV intensity, as at higher values, a PMPC gel formed via homopolymerization of the MPC, resulting in the formation of cracks at the interface of the PMPC layer and the CLPE substrate. When the CLPE was exposed to UV-irradiation during the graft polymerization process, some of its physical and mechanical properties were slightly changed due to cross-linking and scission effects in the surface region; however, the results of all of the tests exceed the lower limits of the ASTM standards. Modification of the CLPE surface with the hydrophilic PMPC layer increased lubrication to levels that match articular cartilage. The highly hydrated thin PMPC films mimicked the native cartilage extracellular matrix that covers synovial joint surface, acting as an extremely efficient lubricant, and providing high-wear resistance. © 2013 Wiley Periodicals, Inc. J Biomed Mater Res Part A: 00A:000–000, 2013.

Key Words: joint replacement, polyethylene, phosphorylcholine, graft polymerization, photoirradiation

How to cite this article: Kyomoto M, Moro T, Yamane S, Hashimoto M, Takatori Y, Ishihara K. 2013. Effect of UV-irradiation intensity on graft polymerization of 2-methacryloyloxyethyl phosphorylcholine on orthopedic bearing substrate. J Biomed Mater Res Part A 2013: 00A: 000–000.

INTRODUCTION

Total hip arthroplasty (THA) has consistently been one of the most successful joint surgeries to date. Owing to the aging global population, the number of primary and revised THAs increases significantly year on year.[1] However, the incidence of osteolysis greatly limits the duration and clinical outcome of this type of surgery.[2,3] Osteolysis is triggered by a host inflammatory response to wear particles produced at the bearing interface of the artificial joint. A typical device consists of cross-linked polyethylene (CLPE) acetabular liner and a cobalt–chromium–molybdenum (Co–Cr–Mo) alloy femoral head, particles of which undergo phagocytosis by macrophages and induce the secretion of bone resorptive cytokines.[4,5] Efforts to reduce the number of these particles and increase the longevity of artificial hip joints have focused on a number of bearing alternatives and improvements to the currently used materials.[6–11] The use of a hard-on-hard THA, such as a metal-on-metal bearing, has been proposed to reduce the wear. However, this has raised new concerns regarding adverse local and systemic effects of metal ion release and electrochemical corrosion, which could cause serious problems such as local soft tissue reactions and pseudotumor formation.[12]

Correspondence to: K. Ishihara; e-mail: ishihara@mpc.t.u-tokyo.ac.jp
Contract grant sponsor: Health and Welfare Research Grants for Research on Medical Devices for Improving Impaired QOL; contract grant number: H20-004
Contract grant sponsor: Research on Publicly Essential Drugs and Medical Devices, Japanese Ministry of Health, Labour and Welfare; contract grant number: H23-007

The bearing surfaces of a natural synovial joint are covered with a specialized type of hyaline cartilage, termed articular cartilage, which protects the joint interface from mechanical wear and facilitates a smooth motion of joints during daily activity.[13,14] Articular cartilage consists of chondrocytes surrounded by extracellular matrix macromolecules (e.g., proteoglycans, glycosaminoglycans, and collagens) and surface active phospholipids (e.g., phosphatidylcholine derivatives). Owing to the charge on these molecules, they can trap water to maintain the water–fluid and electrolyte balance within the articular cartilage tissue, making it highly hydrophilic and providing an effective boundary lubricant.[14,15] The fluid thin-film lubrication achieved by the presence of this hydrated layer is essential for the smooth motion of natural synovial joints. Learning from and mimicking nature has been shown to be a highly successful approach to producing artificial tissues and implants. Therefore, the strategy of investigating and then reproducing the natural bearing surfaces in artificial joints in order to mimic the role of cartilage has great potential.

In this study, we produced nanometer-scale hydrophilic layers composed of 2-methacryloyloxyethyl phosphorylcholine (MPC) on the CLPE surface of an artificial hip joint, with the aim of reducing wear and avoiding bone resorption. Modification of the bearing surfaces of an artificial joint with a hydrophilic layer should increase lubrication to levels that match articular cartilage under physiological conditions. MPC is commonly used to synthesize highly hydrophilic and antibiofouling polymer biomaterials.[16–22] Polymers based on this structure have great potential in the fields of biomedical science and bioengineering because they possess beneficial properties such as excellent antibiofouling ability and low friction. Thus, several medical devices, including intravascular stents,[19] soft contact lenses,[20] artificial hearts,[21] and artificial hip joints,[22] have been developed from MPC polymers and subsequently clinically applied. The biomedical efficacy and safety of MPC polymers are therefore well established. In this study, the nanometer-scale surface modification was accomplished using a photoinduced (i.e., ultraviolet (UV) irradiation) radical polymerization technique[23] similar to the "grafting from" method. This approach has an advantage in that it facilitates the synthesis of both semi-dilute and high-density polymer brushes.[24] This is in contrast to photoinitiated cross-linking and scission reactions of polyolefins, which are similarly used.[25,26] When polyolefins are exposed to UV-irradiation under the radical graft polymerization processing, the effect would be a result of complicated combination of different processes.

In the present study, we investigated the effect of different intensities of UV-irradiation on the extent of photopolymerization of MPC to form a poly(MPC) (PMPC) layer on a CLPE substrate. Such investigations are of great importance in the design of life-long artificial joints, and for obtaining better understanding of their lubrication and wear mechanisms. Here, we evaluated whether UV-irradiation intensity would affect the extent of the PMPC grafting and the properties of the CLPE substrate. In addition, we assessed the potential of the PMPC-graft and/or its layer characteristics for improving the durability of artificial hip joints.

MATERIALS AND METHODS

Graft polymerization with different UV-irradiation intensities

A compression-molded polyethylene (PE; GUR1020 resin; Quadrant PHS Deutschland GmbH, Vreden, Germany) bar stock was irradiated with a 50 kGy dose of gamma rays in a N_2 gas atmosphere, and annealed at 120°C for 7.5 h in N_2 gas in order to facilitate cross-linking. The resulting CLPE specimens were then machined from this bar stock after cooling.

The CLPE specimens were immersed in acetone (Wako Pure Chemical Industries, Ltd., Osaka, Japan) containing 10 mg/mL benzophenone (Wako Pure Chemical Industries) for 30 s, and then dried in the dark at room temperature in order to remove the acetone. MPC was industrially synthesized using the method reported by Ishihara et al. and supplied by NOF Corp. (Tokyo, Japan).[16] The MPC was dissolved in degassed pure water to a concentration of 0.5 mol/L. Subsequently, the benzophenone-coated CLPE specimens were immersed in the MPC aqueous solutions. Photoinduced graft polymerization was carried out on the CLPE surface using UV irradiation (UVL-400HA ultra-high pressure mercury lamp; Riko-Kagaku Sangyo, Funabashi, Japan) with an intensity of 1.5–15 mW/cm^2 at 60°C for 90 min; a filter (model D-35; Toshiba, Tokyo, Japan) was used to restrict the passage of UV light to a wavelengths of 350 ± 50 nm. After the polymerization, the PMPC-grafted CLPE specimens were removed, washed with pure water and ethanol, and dried at room temperature.

Surface analyses

The PMPC-grafted CLPE samples obtained using the range of UV-irradiation intensities were stained using an aqueous solution of 200 ppm (mass) rhodamine 6G (Wako Pure Chemical Industries) because it rapidly associates with the MPC polymer, which is structurally highly similar to lipids.[27] The PMPC-grafted CLPE samples were immersed in the rhodamine 6G solution for 30 s and then washed twice with distilled water for 30 s, and dried. All the samples were examined and imaged using fluorescence microscopy (Axioskop 2 Plus; Carl Zeiss AG, Oberkochen, Germany). Pseudo-color images were obtained using a charge-coupled device (CCD) camera (VB-7010; Keyence, Osaka, Japan) and imaging software (VH analyzer 2.51; Keyence Co.). Lenses with a ×10 magnification and an appropriate exposure time (~0.1 s) were employed to obtain clear images of the samples.

The surface phosphorus concentration of the PMPC-grafted CLPE samples were analyzed using X-ray photoelectron spectroscopy (XPS) using an AXIS-HSi165 spectrometer (Kratos/Shimadzu Co., Kyoto, Japan) equipped with a 15 kV Mg-Kα radiation source at the anode. The take-off angle of the photoelectrons was maintained at 90°, and the P 2p peak was used for phosphorus quantification. Six specimens of each of the PMPC-grafted CLPE samples were prepared, and each sample was scanned five times.

Cross-sectional observations by transmission electron microscopy

Cross-sections of each of the PMPC-grafted CLPE samples were observed using transmission electron microscopy (TEM). The specimens were embedded in epoxy resin, stained with ruthenium oxide vapor at room temperature, and finally sliced into ultra-thin films (approximately 100 nm thick) using a Leica Ultra Cut UC microtome (Leica Microsystems, Wetzlar, Germany). A JEM-1010 electron microscope (JEOL, Tokyo, Japan) was used for the TEM observations at an acceleration voltage of 100 kV. The thickness of the PMPC layer was determined by averaging 10 points on each cross-sectional TEM image.

Wettability and friction tests

Static-water contact angles were measured on each of the PMPC-grafted CLPE samples by employing the sessile drop method using an optical bench-type contact angle goniometer (Model DM300; Kyowa Interface Science, Saitama, Japan). Drops of purified water (1 μL) were deposited on the PMPC-grafted CLPE surfaces, and the contact angles were directly measured after 60 s using a microscope. Fifteen areas were evaluated for each sample, and average values were calculated.

Unidirectional friction tests were performed using a ball-on-plate machine (Tribostation 32; Shinto Scientific, Tokyo, Japan). Six samples of PMPC-grafted CLPE for each irradiation intensities were evaluated. Each specimen was either left non-sterilized or was sterilized by 25 kGy gamma-rays in N_2 gas. A 9 mm diameter pin made from Co–Cr–Mo alloy was also prepared. The surface roughness (R_a) of the pin was <0.01, which was comparable with that of currently used femoral head products. The friction test was performed for each specimen at room temperature using a load of 0.98 or 9.8 N (contact stress roughly calculated by Hertzian theory was ~29 or 62 MPa, respectively), a sliding distance of 25 mm, and a frequency of 1 Hz. A maximum of 100 cycles were carried out, and pure water was used for lubrication. The mean dynamic coefficients of friction were determined by averaging the values of five data points taken from the 96–100 cycles.

Evaluation of physical properties

The swelling ratio and cross-link density of the PMPC-grafted CLPE substrates obtained with various UV-irradiation intensities were evaluated according to previously reported methods.[28] Each of the PMPC-grafted CLPE specimens (23 × 23 × 1 mm) was divided into three sample pieces. The specimens were weighed (approximately 0.5 g, V_1), allowed to swell for 72 h in *p*-xylene containing 0.5 mass% 2-*t*-butyl-4-methylphenol at 130°C, and then reweighed (V_2). The samples were then immersed in acetone, dried at 60°C under vacuum, and weighed again (V_3). The swelling ratio was determined from the weight gain and densities of the PE and xylene, and the physical properties were calculated as follows:

(a) Swelling ratio (q):

$$q = V_2/V_3 \tag{1}$$

(b) Cross-link density:

$$v^* = In(1 - q^1) + q^1 + \chi q^2/V_1\left(q^{-2/3} - 0.5q^{-1}\right) \tag{2}$$

where v^* is the network chain density, $V_1 = 136$ mL/mol, and $\chi = 0.37$ (for PE)

$$M_c = 1/\overline{M}c = Vv* \tag{3}$$

where M_c is the molecular weight between cross-links, and $V = 1$/specimen density.

$$XLD = M_0/\overline{M}c \tag{4}$$

where XLD is the cross-link density, and $M_0 = 14$ (PE)

Mechanical tests

The mechanical properties of the PMPC-grafted CLPE substrates were evaluated using a series of tests. Tensile testing was performed according to ASTM D638 using type IV tensile bar specimens of 1.0 and 2.0 mm in thickness, and a crosshead speed of 50.8 mm/min. Each of the PMPC-grafted CLPE specimens was divided into ten sample pieces, with each evaluated individually. Shore hardness (D) was measured according to the ASTM D2240 test method, with five samples tested for each UV intensity. A double-notched (notch depth = 4.57 ± 0.08 mm) Izod impact test was performed to ASTM F648 standard, with six samples tested for each UV intensity. A small punch test was performed according to ASTM F2183, using a disk specimen of diameter 6.4 mm and thickness 0.5 mm, and a crosshead speed of 0.5 mm/min. Ten sample pieces were evaluated for each UV intensity.

Hip simulator wear test

A 12-station hip simulator (MTS Systems Corp., Eden Prairie, MN) using untreated CLPE and the PMPC-grafted CLPE liners with an inner and outer diameter of 26 and 52 mm, respectively, was used for the wear test according to ISO 14242-3. PMPC-grafted CLPE liners were obtained using UV-irradiation intensities of 1.5, 5.0, and 15 mW/cm^2 and subsequently subject to hip simulator wear test. Three samples of each of the untreated CLPE and the PMPC-grafted CLPE liners were prepared. A Co–Cr–Mo alloy ball 26 mm in diameter (K-MAX® HH-02; KYOCERA Medical Corp., Osaka, Japan) was used as the femoral head. A mixture of 25 vol % bovine serum, 20 mmol/L ethylene diamine tetraacetic acid (EDTA), and 0.1 mass % sodium azide was used as the lubricant. The lubricant was replaced every 5.0 × 10^5 cycles. Gait cycles were applied to simulate a physiological loading curve (Paul-type) with double peaks at 1793 and 2744 N, and a multidirectional (biaxial and orbital) motion of 1 Hz frequency. Gravimetric wear was determined by weighing the liners at intervals of 5.0 × 10^5 cycles. Load-soak controls ($n = 2$) were used to compensate for

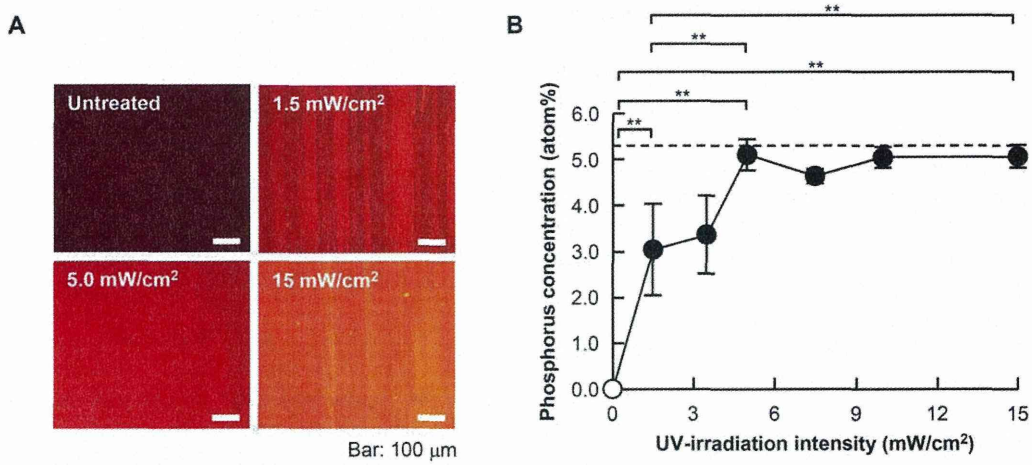

FIGURE 1. (A) Fluorescence microscopy images of rhodamine-stained samples and (B) phosphorus concentrations on PMPC-grafted CLPE surfaces obtained with various UV-irradiation intensities, as calculated using XPS. Open mark indicates untreated CLPE. Data are expressed as mean ± standard deviation. ** indicates $p < 0.01$. Broken lines indicate the theoretical elemental composition (5.3 atom%) of PMPC. [Color figure can be viewed in the online issue, which is available at wileyonlinelibrary.com.]

fluid absorption by the specimens, according to ISO 14242-2. Testing was continued for a total of 5.0×10^6 cycles. Because the gravimetric method was used, the weight loss of each of the tested liners was corrected by subtracting the weight gain due to the load-soak control. However, this correction was not considered to be perfect because only the tested liners were continuously moved and subjected to the load.

The wear particles were isolated from the bovine serum solution, which was then used as a lubricant in the hip joint simulator wear test. To isolate the wear particles, the lubricant was incubated in a 5 mol/L sodium hydroxide solution for 3 h at 65°C to digest adhesive proteins that were degraded and precipitated. In order to avoid artifacts, the contaminating proteins were removed by extraction with solutions of several densities: sugar solution, 1.20 g/cm^3 and 1.05 g/cm^3; and isopropyl alcohol solution, 0.98 g/cm^3 and 0.90 g/cm^3. This was followed by centrifugation at 2.55×10^4 rpm for 3 h at 5°C (himac CP 70MX; Hitachi Koki, Tokyo, Japan). The collected solution was sequentially filtered through a 0.1-μm membrane filter, and the membrane was observed under an FE-SEM (JSM-6330F; JEOL DATUM, Tokyo, Japan) at an acceleration voltage of 20 kV after gold deposition.

In addition, after 5.0×10^6 cycles of the hip simulator wear test, the volumetric wear of the liners was evaluated using a three-dimensional (3D) coordinate measurement machine (BHN-305; Mitutoyo Corp., Kawasaki, Japan). The structures were then reconstructed using 3D modeling software (Imageware; Siemens PLM Software Inc., Plano, TX). To evaluate the wear conditions, the features of the bearing surfaces of the liners were observed using a confocal laser scanning microscope (OLS1200; Olympus Corp., Tokyo, Japan).

Statistical analyses

The mean values of the three or four groups (untreated CLPE and PMPC-grafted CLPE obtained with UV-irradiation intensities of 1.5, 5.0, and 15 mW/cm^2) were compared by one-factor analysis of variance (ANOVA), and the significance of differences of the all comparable properties were determined by post-hoc testing using the Bonferroni method. The dynamic coefficients of friction (ball-on-plate friction test) of PMPC-grafted CLPE with and without gamma-ray sterilization were evaluated using a Student's *t*-test. All the statistical analyses were performed using an add-on (Statcel 2; OMS Publishing, Tokorozawa, Japan) to Microsoft Excel® 2003 (Microsoft Corp., Redmond, WA).

RESULTS

The UV-irradiation intensity was found to affect the extent of PMPC grafting, including the surface phosphorous concentration and the graft layer thickness. As can be seen from the images of rhodamine-treated surface in Figure 1(A), at all irradiation intensities, a PMPC graft layer was formed on the CLPE substrate. The brightness of the uniform fluorescent staining can be seen to increase with UV-irradiation intensity, indicating an increase in the amount of PMPC present. The multiple lines that can be observed on the fluorescence microscopic images are machining marks from cutting of the CLPE bar stock. The phosphorous concentrations of PMPC-grafted CLPE surface, as measured using XPS, increased with the UV-irradiation intensity, and became almost constant at 5.0 atom% over 5.0 mW/cm^2 [Fig. 1(B)]. These values were almost equal to the theoretical elemental composition (5.3 atom%) of PMPC, indicating that the PMPC graft layer fully covered the CLPE substrate. For the samples prepared with UV-irradiation intensities of 1.5 and 5.0 mW/cm^2, a PMPC graft layer 80–150 nm thick can be clearly observed on the surface of the CLPE substrate in the cross-sectional TEM images shown in Figure 2(A). The PMPC-graft layer thickness linearly increased with UV-irradiation intensity, achieving a layer ~380 nm thick at 15 mW/cm^2 [Fig. 2(B)]. However, as can be seen in the TEM image in Figure 2(A) a crack was observed at the

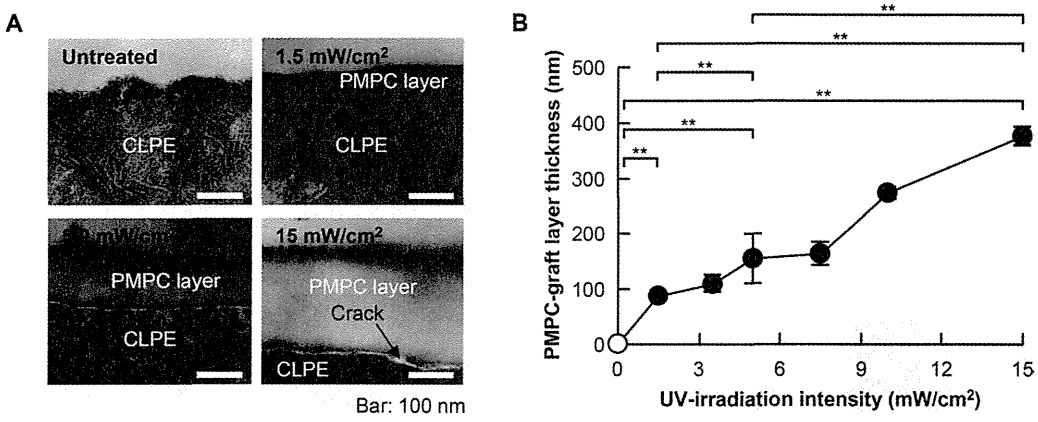

FIGURE 2. (A) Cross-sectional TEM images and (B) PMPC-graft layer thickness of PMPC-grafted CLPE obtained with various UV-irradiation intensities. Open symbol indicates untreated CLPE. Data are expressed as mean ± standard deviation. ** indicates $p < 0.01$.

interface of the PMPC layer and CLPE substrate when a thick polymer layer was formed.

The UV-irradiation intensity affected the hydration and friction kinetics of the PMPC graft layer. The static water contact angle of the untreated CLPE was ~90°, and decreased noticeably with an increase in the UV-irradiation intensity [Fig. 3(A)]. The lowest contact angle observed 30°, which was measured on the samples that was treated at 5.0 mW/cm^2. The angle then increased slightly at higher irradiation intensity. The dynamic coefficients of friction of PMPC-grafted CLPE decreased markedly with an increase in the UV-irradiation intensity, with the surface produced at 3.5–7.5 mW/cm^2 exhibiting an ~85% reduction compared with the untreated CLPE surface [Fig. 3(B)]. However, above 10 mW/cm^2, the values increased slightly. As shown in Figure 4, the dynamic coefficients of friction of the PMPC-grafted CLPE samples obtained using UV-irradiation intensities of 1.5 and 5.0 mW/cm^2 did not differ greatly between loadings, regardless of whether they were gamma-ray sterilized or not. Interestingly, for the nonsterilized PMPC-grafted CLPE obtained with a UV-irradiation intensity of 15 mW/cm^2, the dynamic coefficient of friction in the case of 9.8 N loading was twice as high as that in the case of 0.98 N loading; however, there was no significant difference for the gamma-ray sterilized sample ($p > 0.05$).

Some physical and mechanical properties of PMPC-grafted CLPE as a function of the UV-irradiation intensity are summarized in Figures 5–7. The swelling ratio was almost constant up to an intensity of 10 mW/cm^2, and then decreased slightly above this value [Fig. 5(A)]. The trend in cross-link density also underwent a change at 10 mW/cm^2, gradually increasing up to 0.87 mol % at this point, and then decreasing sharply [Fig. 5(B)]. The ultimate tensile strength and elongation of the untreated CLPE sample differed slightly to the values obtained for the PMPC-grafted CLPE obtained using UV-irradiation intensities of 5.0 and 15 mW/cm^2 [Fig. 6(A,B)]. In contrast, the hardness and impact strength remained almost the same ($p > 0.05$), and appeared to be independent of the UV-irradiation intensity [Fig. 6(C,D)]. The tensile, hardness, and impact resistance properties of all untreated CLPE and PMPC-grafted CLPE samples met the requirements of ASTM F648. The small punch peak strength and work to failure of PMPC-grafted CLPE gradually decreased slightly with UV-irradiation intensity (Fig. 7).

The characteristics of the PMPC-grafted surface affected the durability of the CLPE liners. During the hip simulator

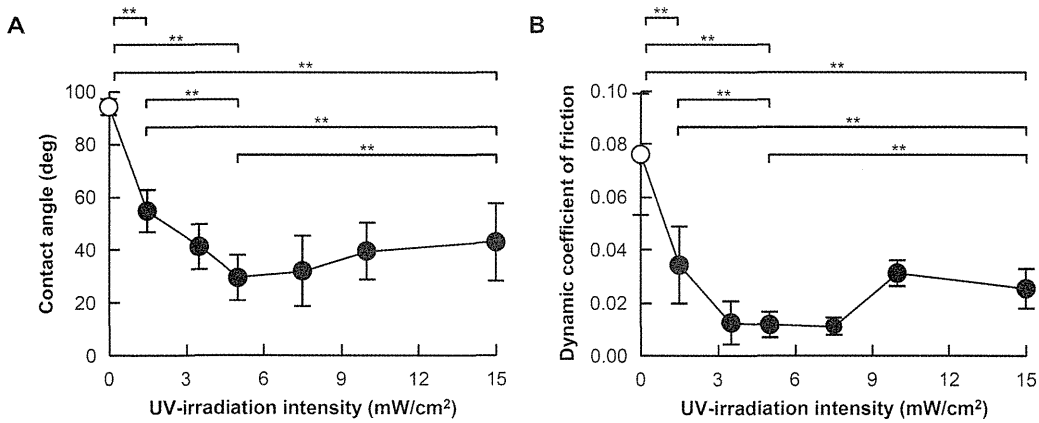

FIGURE 3. (A) Static water contact angle and (B) dynamic coefficient of friction of PMPC-grafted CLPE as a function of the UV-irradiation intensity. Open symbols indicate untreated CLPE. Data are expressed as mean ± standard deviation. ** indicates $p < 0.01$.

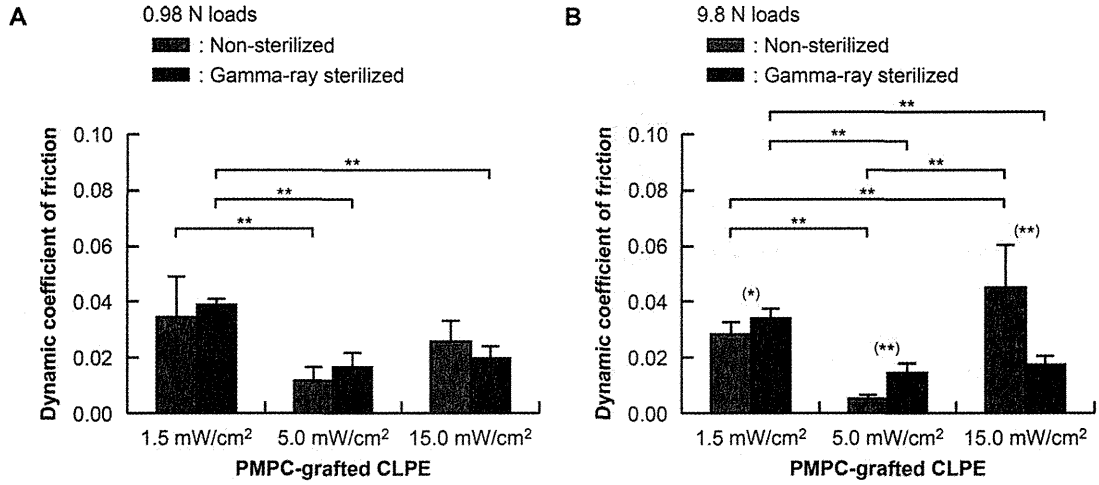

FIGURE 4. Dynamic coefficients of friction of PMPC-grafted CLPE in the ball-on-plate friction test with (A) 0.98 N and (B) 9.8 N loads. Data are expressed as mean ± standard deviation. (*) and (**): *t*-Test, significant differences ($p < 0.05$ and $p < 0.01$, respectively) as a comparison between non-sterilized and gamma-ray sterilized groups, and **: one-factor ANOVA and post-hoc test, significant difference ($p < 0.01$) as comparison between the three groups of the PMPC-grafted CLPE.

wear test, the PMPC-grafted CLPE liner was observed to undergo significantly less gravimetric wear than the untreated CLPE liners [Fig. 8(A)]. Furthermore, there was a slight and gradual increase in weight of the untreated and PMPC-grafted CLPE liners during the testing period, which was partially attributed to greater fluid (e.g., water, proteins, and lipids) absorption by the tested liners than was allowed for by the load-soak controls. As noted earlier, correction using the load-soak control is not perfect because only the tested liners were continuously moved and loaded. Remarkably, extremely small and barely observable wear particles were produced by the PMPC-grafted CLPE liners after 5.0×10^6 cycles ($4.5–5.0 \times 10^6$ cycles) of the hip simulator test [Fig. 8(B)]. The wear particles of the untreated CLPE liners, and the small quantity produced by the PMPC-grafted CLPE, consisted of only sub-micrometer-sized granules. The PMPC grafting did not affect the morphologies of the CLPE wear particles. 3D coordinate measurements of the PMPC-grafted CLPE liners revealed barely detectable volumetric wear, in contrast to the substantial wear detected for the untreated CLPE liners [Fig. 9(A)]. The volumetric wear images in Figure 9(A) are in agreement with the gravimetric wear data shown in Figure 8(A). In the confocal laser scanning microscope images in Figure 9(B), the surface of the untreated CLPE liner against the Co–Cr–Mo alloy femoral head appears smooth. In contrast, the PMPC-grafted CLPE liners exhibit a different morphology; with the machining marks still evident in the bearing surface. There were no differences among the surface morphologies of the three groups of the PMPC-grafted CLPE produced using different UV-irradiation intensities.

DISCUSSION

In this study, we investigated the effects of varying the UV-irradiation intensity on graft polymerization of MPC. The results provide preliminary evidence that the UV-irradiation intensity affected the extent of PMPC grafting and the underlying CLPE substrate. They also demonstrate that the hydrophilic layer increased lubrication to levels that match articular cartilage, and when grafted onto the acetabular liner surface of a THA prosthesis, caused high wear

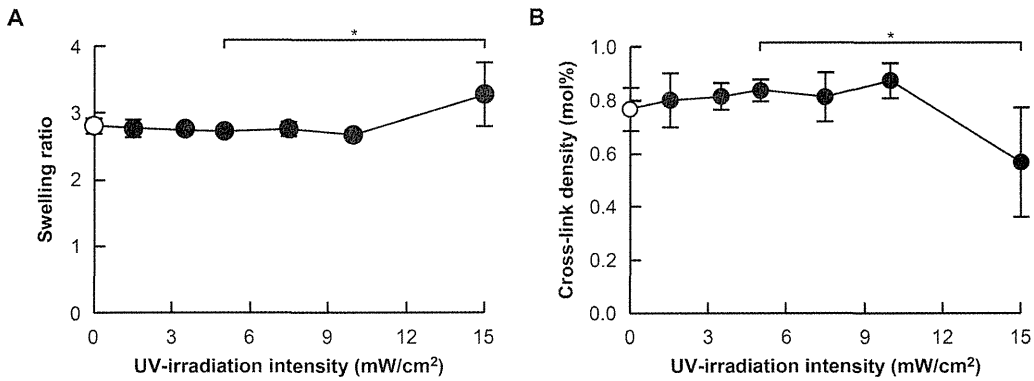

FIGURE 5. (A) Swelling ratio and (B) cross-link density of PMPC-grafted CLPE as a function of UV-irradiation intensity. Open symbols indicate untreated CLPE. Data are expressed as mean ± standard deviation. * indicates $p < 0.05$.